TDA Progress Report 42-112

February 15, 1993



# Performance Results of a 300-Degree Linear Phase Modulator for Spaceborne Communications Applications

N. R. Mysoor and R. O. Mueller
Spacecraft Telecommunications Equipment Section

*A phase modulator capable of large linear phase deviation, low loss, and wideband operation with good thermal stability has been developed for deep space spacecraft transponder (DST) applications at X-band (8.415 GHz) and Ka-band (32 GHz) downlinks. The design uses a two-stage circulator-coupled reflection phase shifter with constant gamma hyperabrupt varactors and an efficient modulator driver circuit to obtain a phase deviation of ±2.5 rad with better than 8 percent linearity. The measured insertion loss is 6.6 dB ±0.35 dB at 8415 MHz. Measured carrier and relative sideband amplitudes resulting from phase modulation by sine wave and square modulating functions agree well with the predicted results.*

## I. Introduction

The telecommunication transponders [1] for Cassini and other future deep space missions require an X-band linear phase modulator. The design is to provide ±2.5 rad of peak phase deviation to accommodate downlink modulation of telemetry and ranging signals. The tolerance on the phase deviation linearity is 8 percent. The phase modulator design specifications [2] for the deep space transponder applications are listed in Table 1. The modulator design concepts, development, analysis, and measured results are presented in this article. The description of the breadboard phase modulator is presented in Section II, the test data and analysis are presented in Section III, and the conclusions are presented in Section IV.

## II. Description of the Phase Modulator

The X-band phase modulator is designed as a cascaded two-stage circulator-coupled reflection phase shifter [2,3,4] with constant gamma hyperabrupt varactors. The gallium arsenide (GaAs) varactor diode is well suited for the phase modulator application as it can provide rapid phase change with the applied voltage. The diode capacity parameter, gamma ($\Gamma$), is the slope of the capacitance–voltage curve as plotted on log–log paper. The gamma of a typical hyperabrupt varactor varies widely with applied voltage, which makes these varactors unsuitable for linear phase-modulator applications. Recent device processing developments [4] have enabled the construction of varactors with gammas that remain constant over a limited voltage bias

range. The GaAs varactors[1] used in this investigation have a constant gamma equal to 1.5. The varactor diode is usually modeled as a junction capacitance in series with the resistance of the GaAs substrate and epitaxial layers. The junction capacitance of varactor diodes is modeled as

$$\frac{C_j(V)}{C_0} = \left[1 + \frac{|V|}{\Phi}\right]^{-\Gamma} \quad (1)$$

where $C_j(V)$ is the junction capacitance at reverse bias voltage, $V$. The value $C_0$ is the junction capacitance at $V = 0$, and $\Phi$ is the built-in potential, which is equal to 1.3 V for GaAs.

The series resistance ($R_S$) of varactor diodes can be determined from the measured diode's quality factor, $Q$. The $Q$ factor is a measure of loss in the varactor diode. The expression for $Q$ as a function of the bias voltage, used in the simulation, was obtained by curve fitting the manufacturer's (Microwave Associates') data at 50 MHz:

$$Q(V) = 1538 - 115.6|V| + 118.2|V|^2 + 21.96|V|^3 - 1.683|V|^4 \quad (2)$$

The diode series resistance is then given by

$$R_S(V) = [2\pi \times 50 \times 10^6 \times Q \times C_j(V)]^{-1} \quad (3)$$

A phase modulator consisting of a two-section reflection phase shifter [2] and a driver circuit was breadboarded and tested. The phase modulator photograph and schematic are illustrated in Figs. 1 and 2, respectively. The module is made out of aluminum alloy 6061, which is tin-lead plated to ensure ease of soldering and good electrical conductivity. The size of the module is 81 × 61 × 14.3 mm. The two-section phase shifter layout is etched on a 0.508-mm-thick RT/Duroid 6002 soft substrate of a dielectric constant equal to 2.94. The constant 1.5 gamma varactors[2] are mounted with a contact strip at the end of an optimized 30-ohm, 2.794-mm-wide transformer. The diode capacitance at −4 V is equal to 0.65 pF. The diode package parasitic capacitance and inductance are equal to 0.23 pF and 0.20 nH, respectively. TRAK Microwave 6.35-mm micropuck circulators [79*9001] and isolators [89*9001] are used in this breadboard. The driver circuit is etched on 0.787-mm-thick RT/Duroid 5880, which has a dielectric constant of 2.2. The phase modulator driver circuit schematic is shown in Fig. 3. The functions of the phase modulator drive circuit are to sum and amplify the modulation input signals and to provide composite drive voltage to the varactor diodes. The modulation input signals include the spacecraft telemetry, ranging, and differential one-way ranging (DOR) signals. The modulation frequency range is from 1 kHz to 20 MHz. The selected wideband op-amp for this application is Comlinear CLC 505.

## III. Experimental Results

The measured values of phase deviation and insertion loss for the phase modulator are compared with the predicted results in Fig. 4. The predicted results were obtained by the computer microwave computer-assisted-design (CAD) simulation of an extensive circuit model of the circuit schematic shown in Fig. 2. The measurements were conducted using a test RF signal level of +9 dBm. The insertion loss for this unit is 6.35 ±0.25 dB, the phase deviation is ±150 deg, with a linearity better than ±8 percent of a best-fitted straight line (BSL). The varactor bias voltage range is 5 ±3.5 V. The model accurately predicted a linear phase slope of 42 deg/V. The predicted insertion loss, including circulator and isolator losses, is 7.0 ±0.4 dB, which is about 0.65 dB higher than the measured values. The discrepancy in the insertion loss is most likely due to the uncertainty in the measured insertion loss of the circulators and isolators. The insertion loss of these devices was measured in a separate test fixture. Circulators measured in this test fixture had a port-to-port one-way insertion loss of 1 ±0.1 dB. The test fixture is not enclosed and, therefore, has radiation losses which the module does not have. Also, circulators were not epoxied in the test fixture as they are in the module; this will result in higher losses since there is not a solid ground contact. The measured results of the phase modulator are compared with its design specifications in Table 1. The phase modulator meets or exceeds all specifications.

Figure 5 shows the predicted and measured gain versus frequency characteristics of the phase modulator driver circuit at −35 deg C, +25 deg C, and +85 deg C. A separate breadboard was used to test the driver circuit. The measured response is flat and drops only 0.4 dB, from 1 kHz to 20 MHz. The measured 3-dB bandwidths at −35 deg C, +25 deg C, and +85 deg C are 92 MHz, 84 MHz, and 75 MHz, respectively. The measured results are actually better than the Simulation Program with Integrated Circuit Emphasis (SPICE) predicted circuit response using a

[1] The varactors were manufactured by Microwave Associates, MA-46411-126.

[2] Ibid.

conservative circuit model for the op-amp integrated circuit. The model correctly predicted a larger bandwidth at lower temperatures. The dc power consumption with an 8-V peak-to-peak output swing is 112 mW; when no signal is applied, the power consumption is 32 mW.

Sinusoidal and square modulating waveforms were applied to the phase modulator, and their resulting spectra [5,6] were monitored on a calibrated spectrum analyzer. All measurements were performed at 25 deg C and with a carrier frequency of 8415 MHz. Figure 6 shows the resulting spectrum when a sinusoidal modulating wave was applied to the phase modulator. The modulating frequency used is 1 MHz, and the peak modulation index is 2.4 rad.

A comparison of measured and predicted carrier, first, second, and third sideband levels for the case of sinusoidal modulation is shown in Fig. 7. A modulation frequency of 10 MHz was used in the measurements. The peak phase-modulation index, $\beta$, ranges from 0.2 to 2.4 rad in 0.2-rad steps. The predicted relative carrier and sideband levels [6] were computed by evaluating the appropriate Bessel functions of the first kind of order $n$, $J_n(\beta)$. The subscript $n$ is an integer. It represents the carrier for $n$ equal to zero and sidebands for $n$ not equal to zero. The relative carrier level for a given modulation index is determined by evaluating $20\log[|J_0(\beta)|]$. Similarly, the relative sideband levels may be determined by evaluating $20\log[|J_n(\beta)|]$ for $|n| > 0$. Figure 7 shows excellent agreement between theory and measurement for sinusoidal phase-modulating waves. Negligible amplitude modulation distortion was observed in this case.

Figure 8 shows the spectrum that results when a square modulating wave at a frequency of 100 kHz and a peak modulation index of 1.571 rad is applied to the phase modulator. A comparison of measured and predicted carrier, first, third, and fifth sideband levels for the case of square-wave modulation is shown in Fig. 9. A modulation frequency of 100 kHz was used in the measurements. The relative carrier level in decibels is determined [6] by evaluating $20\log[|\cos(\beta)|]$, where $\beta$ is the peak modulation index. The relative sideband levels may be determined [6] by evaluating $20\log[|(2/n\pi)\sin(\beta)|]$ , where $n$ is the number of the sideband. Excellent agreement between predicted and measured square-wave modulation results is demonstrated in Fig. 9.

The data illustrated in Figs. 7 and 9 were obtained by the judicious use of a spectrum analyzer. For small modulation indices, setting the first sideband level is the most accurate way [5] to obtain a particular value of a modulation index. For example, if a modulation index of 0.2 rad (sinusoidal modulation) is needed, then the modulation power level should be adjusted until the first sideband level falls 20.0 dB below the unmodulated carrier level. The error in the measurement is determined by the accuracy of the spectrum analyzer. If the above reading is accurate to within 1 dB, then the modulation index would be accurate to within 0.03 rad. For larger modulation indices, the first sideband will give large errors. In this case, the carrier level should be used to set the modulation index. The decision of whether to use the carrier or the first sideband level can, in general, be made by choosing the one that has the steepest slope [5] near the desired modulation index.

## IV. Conclusions

A two-section analog X-band reflection phase modulator with an efficient driver circuit was developed. The phase modulator performance is accurately predicted by the theoretical modeling and simulations. By using hyperabrupt junction GaAs varactor diodes of a constant gamma of 1.5, a full $\pm 2.5$-rad deviation phase modulator was realized by cascading two phase shifter circuits. An efficient phase modulator driver circuit was also developed and tested. The measured gain-frequency characteristics of the modulator driver circuit over the design temperature range agreed well with the predicted results. The modulator driver 3-dB bandwidth and dc power consumption at 25 deg C are 84 MHz and 112 mW, respectively. At 8415 MHz, the measured phase shift and insertion loss of the phase modulator are equal to $\pm 2.5$ rad, with better than $\pm 8$ percent linearity, and 6.35 $\pm 0.25$ dB, respectively. Measured carrier and sideband spectra showed excellent agreement with theory with negligible amplitude modulation distortion for both sinusoidal and square phase modulating waves.

## Acknowledgments

The authors gratefully acknowledge the valuable support of A. W. Kermode for comments on design and analysis and J. H. Meysenburg for breadboard fabrication and testing.

# References


[1] N. R. Mysoor, J. D. Perret, and A. W. Kermode, "An X-Band Spacecraft Transponder for Deep Space Applications—Design Concepts and Breadboard Performance," *IEEE Trans. Microwave Theory Tech.*, vol. MTT-40, no. 6, pp. 1192–1198, June 1992.

[2] N. R. Mysoor and R. O. Mueller, "Design and Analysis of Low-Loss Linear Analog Phase Modulator for Deep Space Spacecraft X-band Transponder (DST) Application," *The Telecommunications and Data Acquisition Progress Report 42-105, vol. January–March 1991*, Jet Propulsion Laboratory, Pasadena, California, pp. 136–145, May 15, 1991.

[3] R. Garver, "360 deg Varactor Linear Phase Modulator," *IEEE Trans. Microwave Theory Tech.*, vol. MTT-17, pp. 137–147, March 1969.

[4] E. C. Niehenke, V. V. DiMarco, and R. Friedberg, "Linear Analog Hyperabrupt Varactor Diode Phase Shifters," *IEEE 1985 International Microwave Theory and Techniques Symposium*, Digest of papers, pp. 657–660, June 1985.

[5] E. A. Whitman, "Phase Modulation Measurement Techniques for Improved Accuracy," *Microwave Journal*, pp. 113–116, June 1978.

[6] F. Stocklin, *Relative Sideband Amplitudes vs. Modulation Index for Common Functions Using Frequency and Phase Modulation*, Goddard Space Flight Center, distributed by National Technical Information Service, U. S. Department of Commerce, Springfield, Virginia, November 1973.

**Table 1. Measured results and design specifications for the phase modulator.**

| Parameter | Specification | Measurement (25 deg C) |
|---|---|---|
| Insertion loss | 10 dB, max | 6.6 dB, max |
| Amplitude modulation | ±0.5 dB, max | +0.15/−0.35 dB |
| Input return loss | 14 dB, min | 25 dB (8415 ±50 MHz) |
| Output return loss | 14 dB, min | 33 dB (8415 ±50 MHz) |
| RF input level (for linear operation) | +10 dBm, max | +10 dBm, max |
| Linearity | ±5 percent (best straight line) to ±2 rad | +4.8/−3.1 percent |
| Modulation sensitivity | 2 ±0.2 rad/V | 2.1 rad/V |
| Modulation input signal level at ±2.5 rad | ±2.5 V, max | ±1.28 V, max |
| Op-amp gain | — | 2.8 V/V |
| RF modulation bandwidth | | |
| −0.25 dB bandwidth | 20 MHz, min | 28 MHz |
| −3 dB bandwidth | 82 MHz, min | 160 MHz |
| DC power (at 20 MHz and ±2.5 rad) | | |
| +5 V | 25 mA, max | 7.0 mA |
| −5 V | 25 mA, max | 6.9 mA |
| Modulation voltage range (to varactors) | — | −1.5 to −8.5 V |

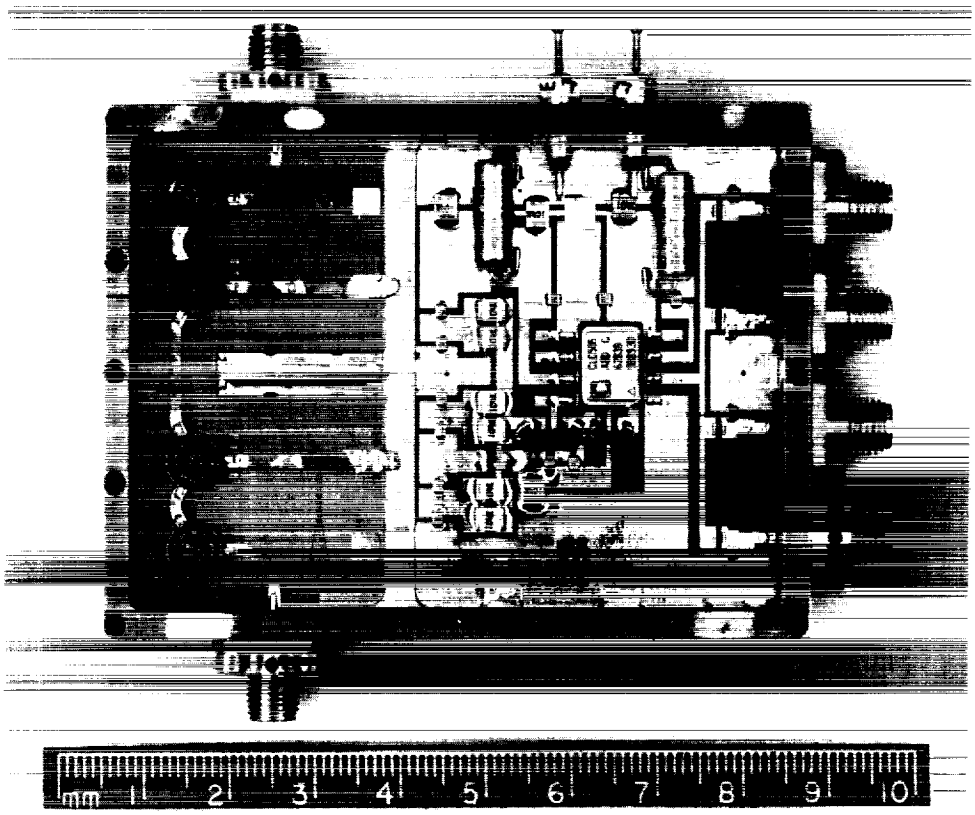


Fig. 1. DST X-band phase modulator and driver circuit assembly.

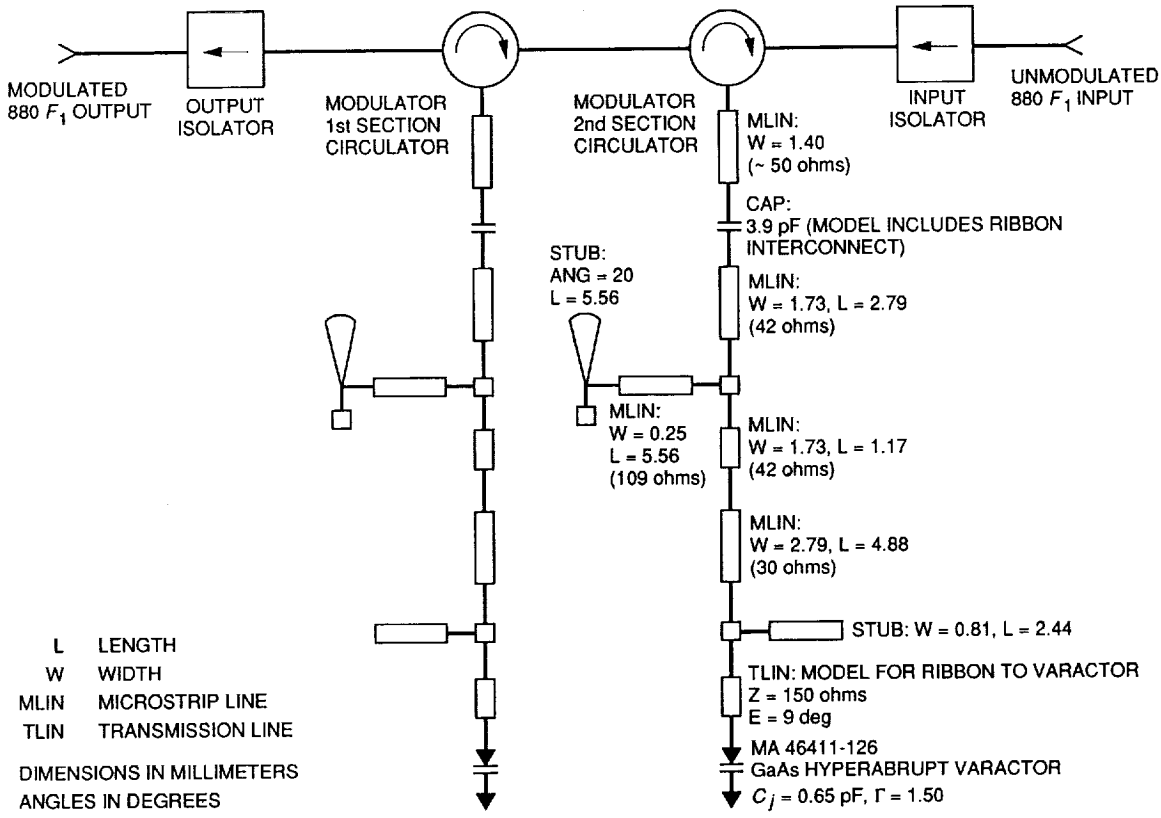


**Fig. 2. DST X-band phase modulator schematic.**

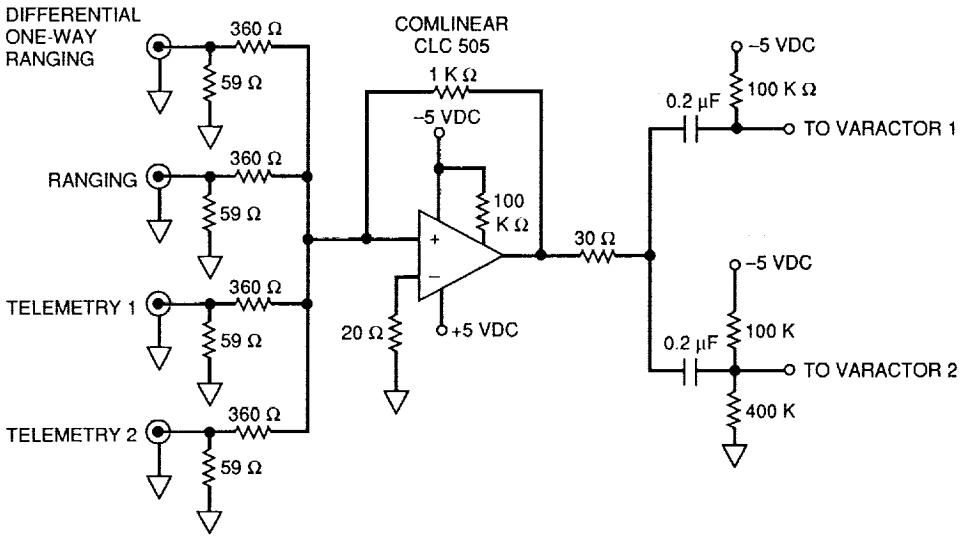


**Fig. 3. DST phase modulator driver circuit schematic.**

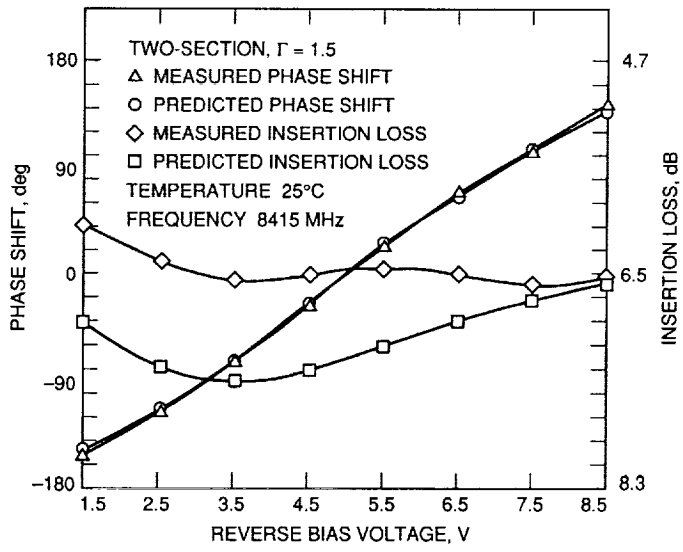


**Fig. 4. Measured and predicted results for the phase modulator.**

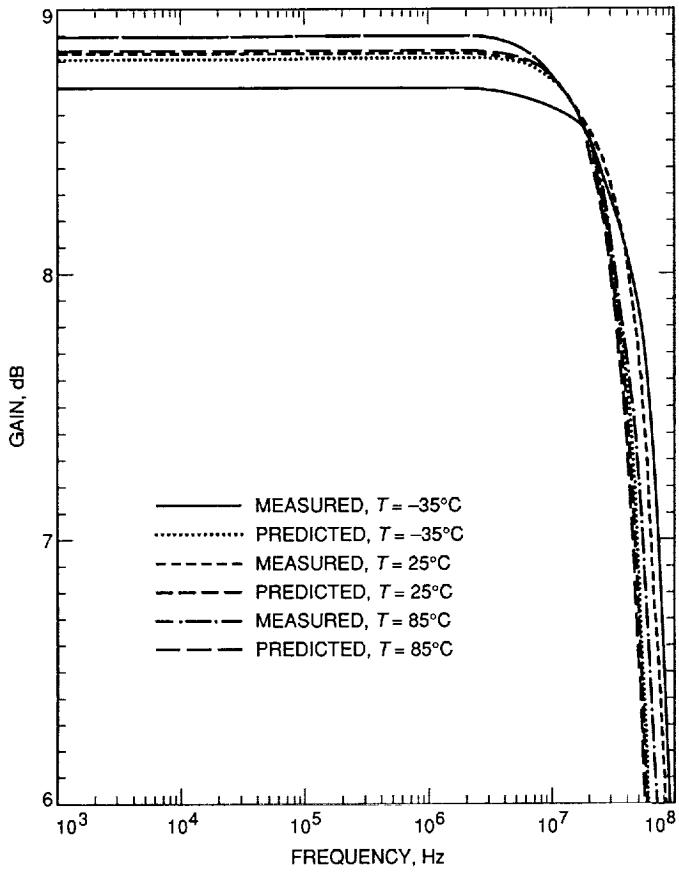


**Fig. 5. Measured and predicted gain versus frequency for the phase modulator driver circuit at temperatures of –35, 25, and 85 deg C.**

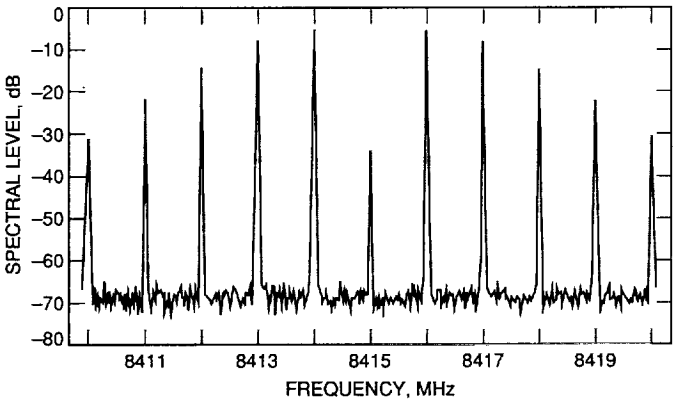


**Fig. 6. Measured phase-modulated spectrum for the case of a sinusoidal modulating wave at a frequency of 1 MHz and a peak modulation index of 2.4 rad.**

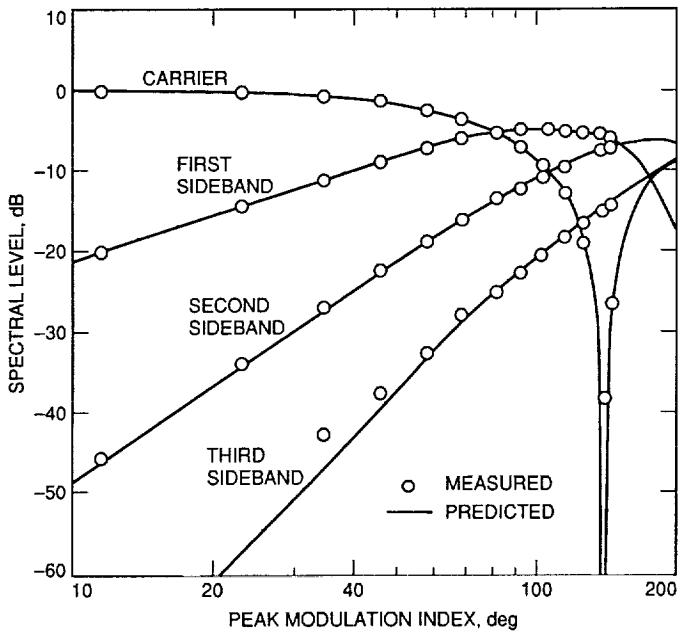


**Fig. 7. Measured and predicted carrier, first, second, and third sideband levels versus peak modulation index for the case of a sinusoidal modulating wave at a frequency of 10 MHz.**

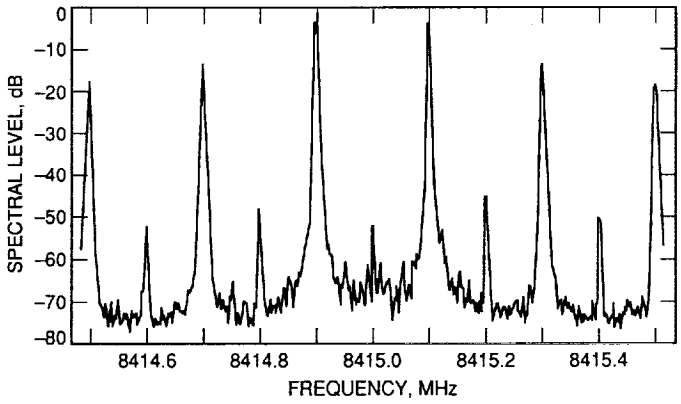


**Fig. 8. Measured phase-modulated spectrum for the case of a square modulation wave at a frequency of 100 kHz and a peak modulation index of 1.571 rad.**

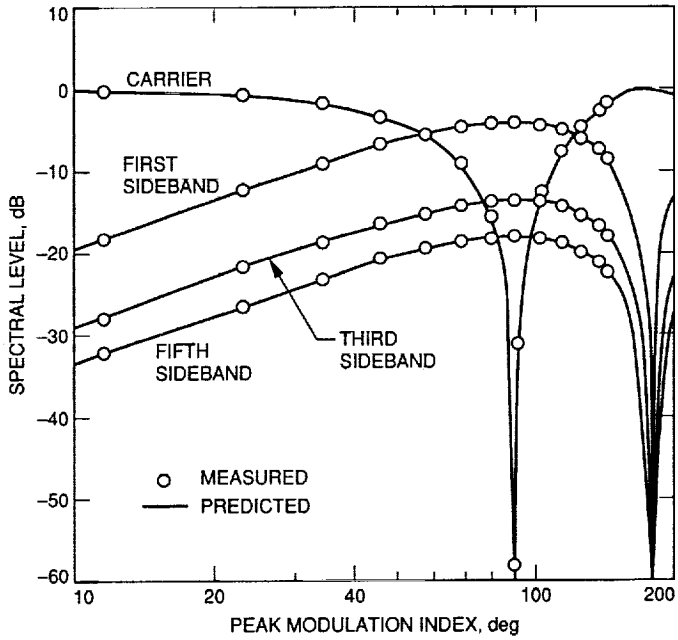


**Fig. 9. Measured and predicted carrier, first, third, and fifth sideband levels versus peak modulation index for the case of a square modulating wave at a frequency of 100 kHz.**